

재활용 폴리프로필렌/아타풀자이트 복합재료의 기계적 및 결정화 특성 개선을 위한 피셔-트롭쉬 왁스(Fischer-Tropsch Wax)의 기능화 변형

Tian-Jiao Zhao[#], Fu-Hua Lin^{*,#}, Shuang-Dan Mao, Ya-Peng Dong, Jia-Le Zhao, Wen-Ju Cui^{**},
Shu-Hui Wang, Ding-Yi Ning, Jing-Qiong Lu, and Bo Wang[†]

School of Chemical Engineering and Technology, Taiyuan University of Science and Technology

^{*}School of Traffic Engineering, Shanxi Vocational University of Engineering Science and Technology

^{**}School of Environment and Resources, Taiyuan University of Science and Technology

(2023년 11월 7일 접수, 2024년 1월 22일 수정, 2024년 1월 29일 채택)

Functionalization Modification of the Fischer-Tropsch Wax to Improve the Mechanical and Crystallization Properties of the Recycled Polypropylene/Attapulgite Composites

Tian-Jiao Zhao[#], Fu-Hua Lin^{*,#}, Shuang-Dan Mao, Ya-Peng Dong, Jia-Le Zhao, Wen-Ju Cui^{**},
Shu-Hui Wang, Ding-Yi Ning, Jing-Qiong Lu, and Bo Wang[†]

School of Chemical Engineering and Technology, Taiyuan University of Science and Technology, Taiyuan 030024, China

^{*}School of Traffic Engineering, Shanxi Vocational University of Engineering Science and Technology, Taiyuan 030619, China

^{**}School of Environment and Resources, Taiyuan University of Science and Technology, Taiyuan 030024, China

(Received November 7, 2023; Revised January 22, 2024; Accepted January 29, 2024)

Abstract: The attapulgite (ATP) with unique one-dimensional rod-like structure was used to improve the mechanical and crystallization properties of the recycled polypropylene (rPP). In order to increase the compatibility of the polar ATP and the non-polar rPP, the maleic anhydride (MAH) was grafted onto the fischer-tropsch wax (FTW) then reacted with ATP to prepare FATP. The tensile, flexural and impact strength of the composites were maximized at the FATP content was 3 wt%, increased by 13.09, 17.56, and 101.92% compared with rPP, and reaching the level of the PP. Due to the improved compatibility, the mechanical properties of the rPP/FATP composites were increased compared with the rPP/ATP composites at the same addition. Moreover, the differential scanning calorimetry (DSC) analysis proved that the addition of the ATP or FATP improved the crystallization properties of the rPP. The crystallization temperature (T_p) of the rPP, rPP/3 wt% ATP, and rPP/3 wt% FATP was 126.31, 127.86, and 129.37 °C, respectively. The non-isothermal and isothermal crystallization kinetic results showed that the crystallization rate was increased with the addition of the ATP and FATP. Meanwhile, by reason of the synergistic effect of compatibility improvement and internal lubrication, the crystallization rate of the rPP/FATP composites was faster than the rPP/ATP composites. However, the ATP or FATP added in rPP had no effect on the spherulites growth mode of the composites. Above all, the scanning electron micrographs (SEM) results provided intuitive evidence which the compatibility between FATP and rPP was greatly improved.

Keywords: recycled polypropylene, attapulgite, fischer-tropsch wax, compatibility, properties.

Introduction

Polypropylene (PP) is characterized by excellent chemical resistance, heat resistance and mechanical properties which has lots of extensive applications in the automotive and aerospace industries.^{1,2} Nevertheless, the limited biodegradability of the

PP contributes to the escalating accumulation of waste which leading to adverse environmental effect.³ Therefore, managing PP waste is crucial to solve environmental problems which include landfills, incineration and recycling.⁴ Landfill may waste valuable resources and cause land occupation, incineration may produce toxic gases and cause pollution. Therefore, recycling PP is the best way to solve sustainability and environmental issues.^{5,6} According to distinct mechanisms, recycled PP (rPP) can be categorized into mechanical recycling and chemical recycling.⁵ Compared with the intricate procedure involved in

[#]These authors contributed equally to this work.

[†]To whom correspondence should be addressed.

wangbo@tyust.edu.cn, ORCID[®]0000-0003-2629-0619

©2024 The Polymer Society of Korea. All rights reserved.

chemical recycling, mechanical recycling is easier to operate and widely adopted method globally.⁷⁻⁹

However, the poor mechanical properties of the rPP obstruct the use of the mechanical recycling.¹⁰ This is because the molecular chains of the rPP are broken during long-term use and multiple processing. The scission chains diminish the presence of ordered segments, leading to the decrease of the crystallization properties of the rPP and subsequently resulting in the reduction of the mechanical properties of the rPP.^{11,12} Blending modification has been widely used in industries to restore the original properties of the rPP, this way refers to blending of polymers with different properties to create high-property polymers, and has advantages of simplicity and cost-effectiveness.^{13,14} There are various additives to melt blending with rPP, including elastomer,¹⁵ biomass fibers¹⁶ and inorganic particles.¹⁷ Among them, inorganic particles which have better heat resistance, higher strength and lower price are extensively used for blending with rPP.¹⁷ This is because inorganic particles can provide heterogeneous nucleation sites for rPP.¹⁸ Then crystals initiate growth from these sites, reducing the time during random movement of molecular chains to form critical nuclei, increasing nucleation density, and improving the crystal structure of the rPP.¹⁹

As a kind of inorganic particles, attapulgite (ATP) has unique one-dimensional rod-like structure which is widely used in blending with pure PP.²⁰ Wang *et al.*²¹ prepared the PP/ATP composites. The results showed that with increased ATP content, the spherulite size of composites decreased and the number increased. Therefore, the crystallization temperature (T_p) increased 5 °C and the impact strength increased 70% compared with pure PP. Chen *et al.*²² found that the PP/4 wt% ATP composites exhibited a notable increase in T_p compared with pure PP, the Young's modulus increased by 812 MPa, and the spherulite size of the composites decreased. In summary, there is a rationale to explore the blending of the ATP and the rPP which has the potential to yield promising results.

However, the ATP with strong polarity and the non-polar rPP cause the poor compatibility of the rPP and ATP which may affect modification effects.²³ Currently, there are lots of methods for improving the compatibility between polar particles and non-polar polymers, including coupling agent treatment, adding compatibilizers, and modification through reactions with long-chain fatty acids.²⁴⁻²⁶ Among them, coupling agent treatment and adding compatibilizers have the advantage of simplicity.^{24,25} The long carbon chain can act as lubricant during the crystallization process of the polymer.²⁶ However, The coupling agent can only treat the surface of inorganic particles, so that the effect is limited. The main composition of the compatibilizers which is used in PP/inorganic particles composites is polypropylene grafted with maleic anhydride (MAPP), but during the preparation process, due to the large molecular weight of the matrix polymer, there is a challenge to obtain higher grafting ratio which may affect the modification effect. The long-chain fatty acids have smaller molecular weight, resulting in less effect compared with compatibilizers. In summary, it is necessary to search a kind of long-chain acids with suitable molecular chain lengths to modify ATP, then achieve the anticipated improvement of the crystallization and mechanical properties of the rPP/ATP composites.

Fischer-tropsch wax (FTW) is a waxy substance composed of C₄₀-C₈₀ straight-chain saturated alkanes.²⁷ The FTW has internal lubrication properties and the carbon chain length is moderate, thus exhibiting excellent effective in improving compatibility.²⁸ In our previous work, the maleic anhydride (MAH) was grafted onto the FTW to obtain fischer-tropsch acid (MAFT) which has acid value of 50 mg KOH/g. The ATP reacted with the MAFT to prepare the FATP, thereby reducing the polarity of the ATP. The FATP was greatly accelerating the crystal transformation rate of the isotactic polybutene.²⁹ The reaction diagram was shown in Figure 1. Besides, the acid value of the MAPP is about 20-30 mg KOH/g which is lower than that of MAFT.³⁰

In this study, to improve the interface compatibility between

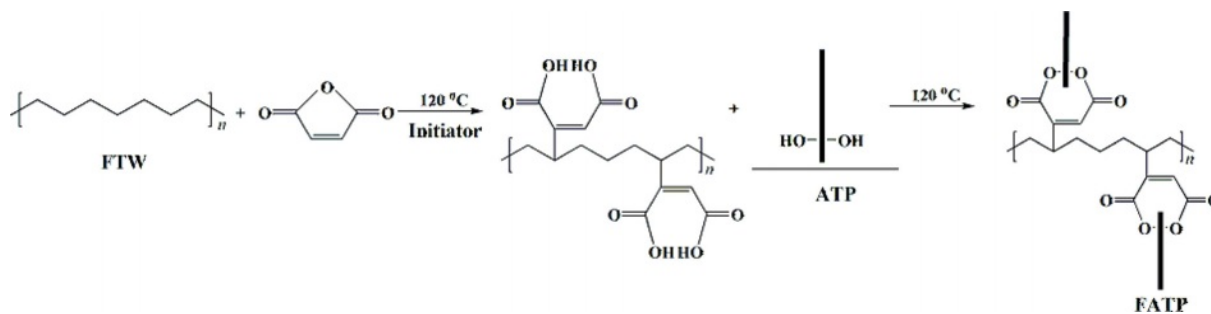


Figure 1. Reaction diagram of the FATP.²⁹

ATP and rPP and use the internal lubrication effect of the MAFT, the ATP was reaction with MAFT to obtain FATP. The ATP and FATP were melting blending with rPP to prepare the rPP/ATP composites. The interface compatibility between ATP and rPP was observed by scanning electron microscopy (SEM). The mechanical properties and the crystallization behavior of the composites were determined in detail. Meanwhile, the crystallization kinetic of the composites was calculated from the *Avrami* equation.

Experimental

Feedstock Sources. The rPP (S1003) and PP (S1003) was supplied by Sinopec Yanshan Company (China). The ATP was purchased from Jiangsu Aotebang Nonmetal Co., Ltd. (China). The synthesis of the FATP which the acid value was 50 mg KOH/g acid has been documented in publications from our previous work.²⁹

Preparation of the rPP/ATP Composites. The formulation of the rPP/ATP composites was shown in Table 1. The samples were mixed with a high-speed mixer (Songqing Hardware Factory, SL-500A, China). The mixed samples were extruded and pelletized by a twin-screw extruder (Shanghai Xinshuo Precision Machinery Co., Ltd. WLG10A, China). The standard test specimens were molded by an injection machine (Shanghai Xinshuo Precision Machinery Co., Ltd. WZS10D, China) with an injection pressure of 15.5 MPa and 180 °C.

Mechanical Properties of the rPP/ATP Composites. The tensile properties of the composites were assessed following the specification of GB/T 1040-2006, utilizing universal testing machine (Jiangsu Tianyuan Test Instrument Co., Ltd. TY-8000A, China) at a speed of 5 mm/min. The flexural tests were performed according to GB/T 9341-2008, utilizing universal testing machine at a speed of 10 mm/min. Impact strength of the composites was measured by impact tester (Jiangsu Tianyuan Test Instrument Co., Ltd. TY-4021, China) with 5.5 J capacity at

maximum pendulum height (150°) at room temperature according to GB/T 1043.1-2008. Five samples were tested individually and the average results were recorded.

Crystallization Behavior Characterization of the rPP/ATP Composites. The crystallization behavior of the composites was performed by DSC (Q1000, TA Instruments Inc., USA) in a nitrogen atmosphere (50 mL/min). All the composites were eliminated the thermal history from 30 to 210 °C at 10 °C/min before testing. For the non-isothermal crystallization behavior, the composites were cooled from 210 to 30 °C at different heating rate (10, 20, 30 °C/min), then heated from 30 to 210 °C at 10 °C/min. For the isothermal crystallization behavior, the composites were cooled from 210 °C to different temperatures (140, 143, 145 °C), maintained the temperature for 35 min. then cooled from different temperatures to 30 °C at 10 °C/min.

SEM of the rPP/ATP Composites. The compatibility between ATP and rPP was investigated by SEM (S4800, Hitachi Ltd., Japan) at an accelerating voltage of 5 kV.

Result and Discussion

Mechanical Properties of the rPP/ATP Composites. Figure 2 illustrated the tensile properties of the composites at different ATP addition. The composites demonstrated an initial increase followed decrease tendency in tensile properties with increased ATP or FATP addition. This was because the appropriate addition of the ATP or FATP can evenly distribute within the rPP, thus improving the tensile properties of the composites. However, the excessive addition of the ATP or FATP tended to aggregate within the rPP due to the effect of intramolecular hydrogen bonds. The aggregation affected the compatibility between ATP and rPP, ultimately leading to the decrease of tensile properties.³¹ The tensile strength and tensile modulus of the composites reach peak values when the ATP or FATP content was 3 wt%. Compared with rPP, the rPP/3 wt% ATP composite increased by 7.31% and 7.85%, while the rPP/3 wt% FATP composite increased by 13.09% and 11.46%, effectively match the properties of the PP. This was because the ATP can act as heterogeneous nucleating agent, promoting the close packing of the composites molecular chains and thereby enhancing the tensile properties of the composites.²¹ The MAFT can react with -OH in ATP to produce FATP, reducing the molecular polarity of the ATP and improving the compatibility between ATP and rPP, thereby achieving better effects.³²

Figure 3 depicted the flexural properties of the composites. With increased ATP addition, the flexural properties demon-

Table 1. Formulation of the rPP/ATP Composites Table

| Sample | rPP (wt%) | ATP (wt%) | FATP (wt%) |
|----------------|-----------|-----------|------------|
| rPP | 100 | - | - |
| rPP/1 wt% ATP | 99 | 1 | - |
| rPP/3 wt% ATP | 97 | 3 | - |
| rPP/5 wt% ATP | 95 | 5 | - |
| rPP/1 wt% FATP | 99 | - | 1 |
| rPP/3 wt% FATP | 97 | - | 3 |
| rPP/5 wt% FATP | 95 | - | 5 |

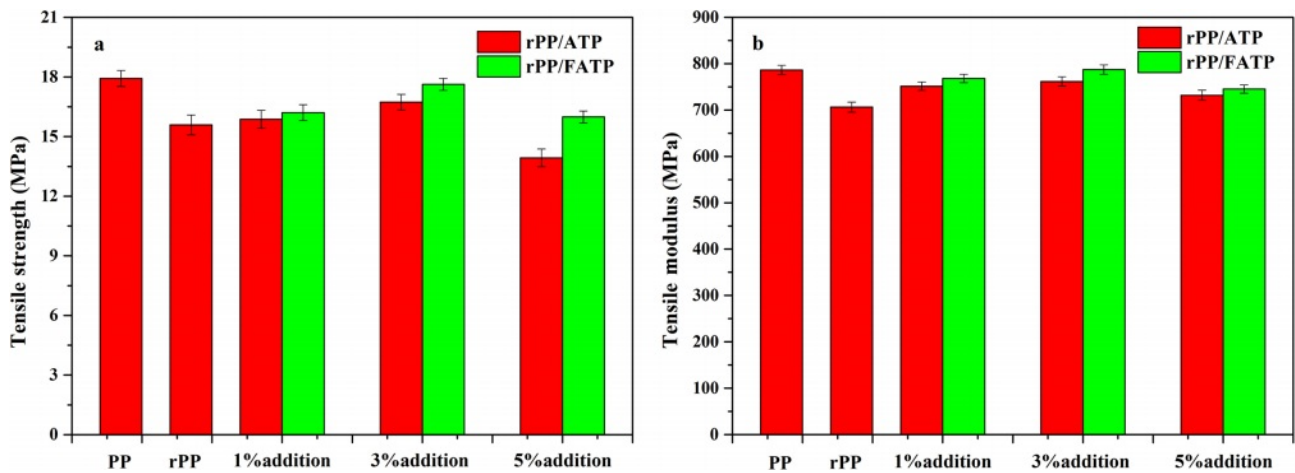


Figure 2. Tensile properties of the rPP/ATP composites: (a) tensile strength; (b) tensile modulus.

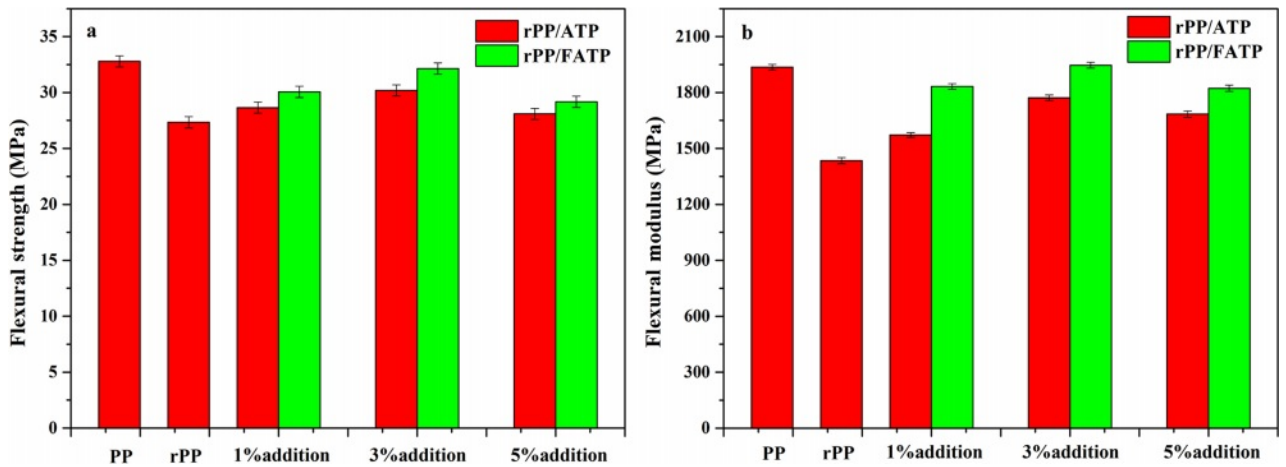


Figure 3. Flexural properties of the rPP/ATP composites: (a) flexural strength; (b) flexural modulus.

Table 2. Non-isothermal Crystallization Kinetic Parameters of the rPP/ATP Composites

| Sample | Φ | T_p ($^{\circ}\text{C}$) | ΔH (J/g) | n | $\log k_c$ | $t_{1/2}$ (min) |
|----------------|--------|------------------------------|------------------|------|------------|-----------------|
| PP | 10 | 129.54 | 81.79 | 3.85 | 0.3198 | 1.79 |
| | 20 | 126.76 | 80.99 | 3.33 | 2.2668 | 1.42 |
| | 30 | 125.11 | 79.79 | 3.08 | 2.5821 | 1.04 |
| rPP | 10 | 126.31 | 53.59 | 3.61 | -0.1239 | 2.23 |
| | 20 | 123.05 | 52.30 | 3.68 | 1.8707 | 1.76 |
| | 30 | 122.82 | 50.52 | 3.32 | 2.4929 | 1.32 |
| rPP/3 wt% ATP | 10 | 127.86 | 50.90 | 3.85 | 0.2534 | 2.01 |
| | 20 | 125.29 | 48.26 | 3.67 | 1.9340 | 1.58 |
| | 30 | 122.83 | 48.07 | 3.10 | 2.8864 | 1.21 |
| rPP/3 wt% FATP | 10 | 129.37 | 49.24 | 3.56 | 0.5139 | 1.80 |
| | 20 | 125.59 | 48.06 | 3.87 | 2.2561 | 1.41 |
| | 30 | 122.43 | 48.23 | 3.17 | 3.1862 | 1.05 |

strated a similar trend to the tensile properties, which was also attributed to aggregation caused by ATP or FATP addition. The

flexural strength and flexural modulus of the composites attained peak values when the ATP or FATP content was 3 wt%. Com-

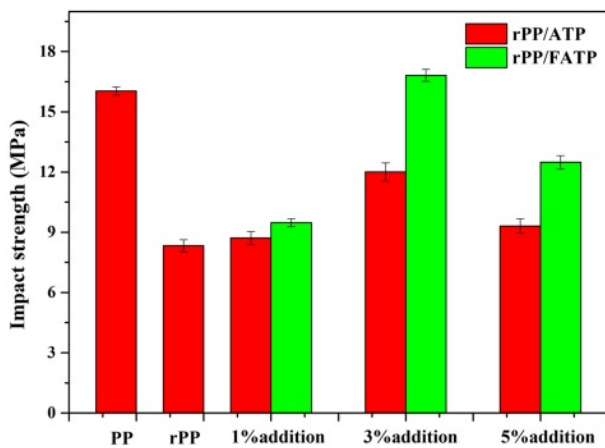


Figure 4. Impact strength of the rPP/ATP composites.

pared with rPP, the rPP/3 wt% ATP composite increased by 10.42% and 23.54%, while the rPP/3 wt% FATP composite increased by 17.56% and 35.32%, effectively matched the properties of the origin PP. This was because the ATP can refine the crystal and reduce the crystal size of the rPP, thereby improving the rigidity of the composites.³³ The MAFT in FATP which had molecular chains of moderate length can improve of com-

patibility and resulted in stronger interface adhesion between FATP and rPP, and that was the reason of the rPP/3 wt% ATP composite had the maximum flexural properties.³⁴

Figure 4 was shown the impact strength of the composites. The trend in impact strength was similar to the tensile and flexural properties which was also attributed to aggregation caused by excessive ATP or FATP addition. At the ATP or FATP content was 3 wt%, the composites reached the maximum impact strength. Compared with rPP, the rPP/3 wt% ATP composite and the rPP/3 wt% FATP composite increased by 44.18% and 101.92%, respectively. This was because the ATP can improve the boundary strength of the spherulites which consequently improving the impact strength of the composites.³⁵ Moreover, the MAFT with moderate carbon chain length can promote ATP to disperse evenly in the rPP matrix.^{29,36} Therefore, compared with ATP, the FATP had better compatibility with the rPP which had higher impact strength.

Non-Isothermal Crystallization Behavior of the rPP/ATP Composites. The non-isothermal crystallization curves for different composites were shown in Figure 5, and the data was shown in Table 2. With increased cooling rates, the T_p of the composites decreased. This was because rapidly changes of

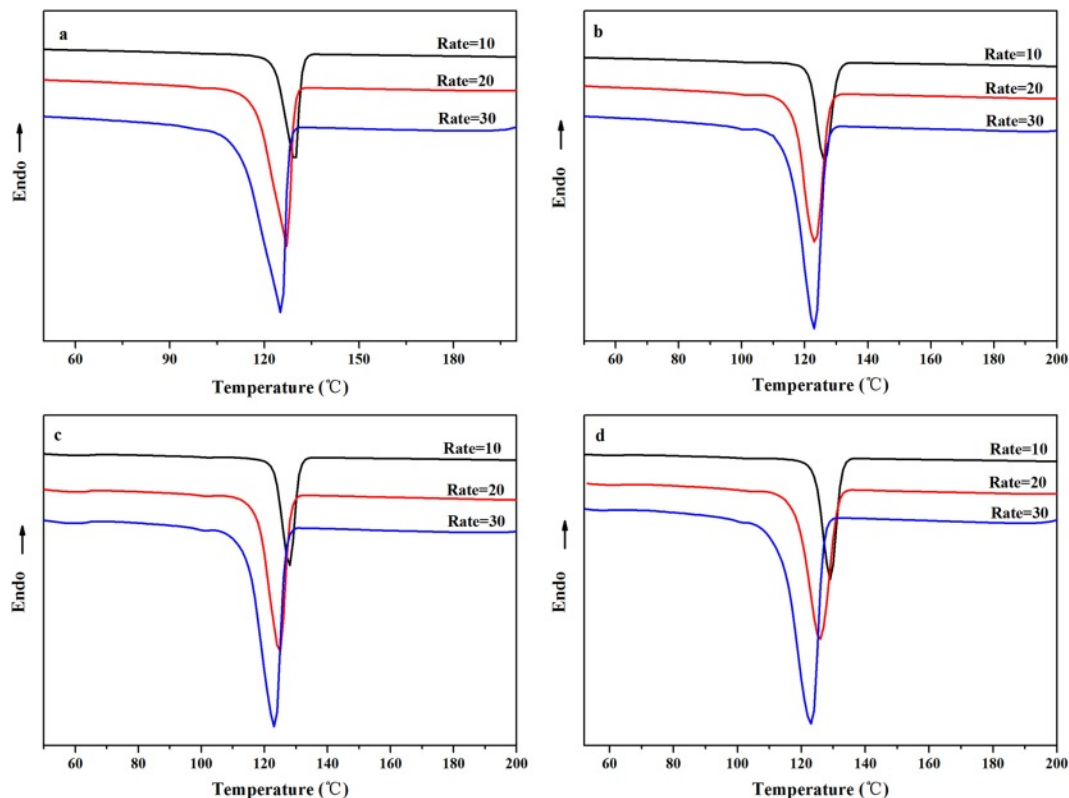


Figure 5. Non-isothermal crystallization curves of the rPP/ATP composites at different cooling rates: (a) PP; (b) rPP; (c) rPP/3 wt% ATP; (d) rPP/3 wt% FATP.

temperature allow insufficient time for molecular chains to align in ordered manner, thereby resulting in decrease in crystallization properties.³⁷

It was evident from Figure 5 and Table 2 that under same cooling rate, The T_p of the composites increased with increased addition, and when the ATP or FATP content was 3 wt%, the composites had the highest T_p . At the cooling rate of 10 °C/min, The T_p value of the rPP, rPP/3 wt% ATP, and rPP/3 wt% FATP were recorded as 126.31, 127.86, and 129.37 °C, and the rPP/3 wt% FATP composite can match the property of the PP. This was because the ATP can provide nucleation sites for the composites, promoting the ordered arrangement of the molecular chains around ATP, thereby increasing the T_p of the composites.²¹ The FAFT can uniform dispersion in the rPP matrix due to good compatibility, and thereby the rPP/FATP had the highest T_p .²³

The relative crystallinity $X(T)$ of the composites was given by eq. (1):

$$X(T) = \int_{T_0}^T \left(\frac{dH}{dT} \right) dT / \int_{T_0}^{T_\infty} \left(\frac{dH}{dT} \right) dT \quad (1)$$

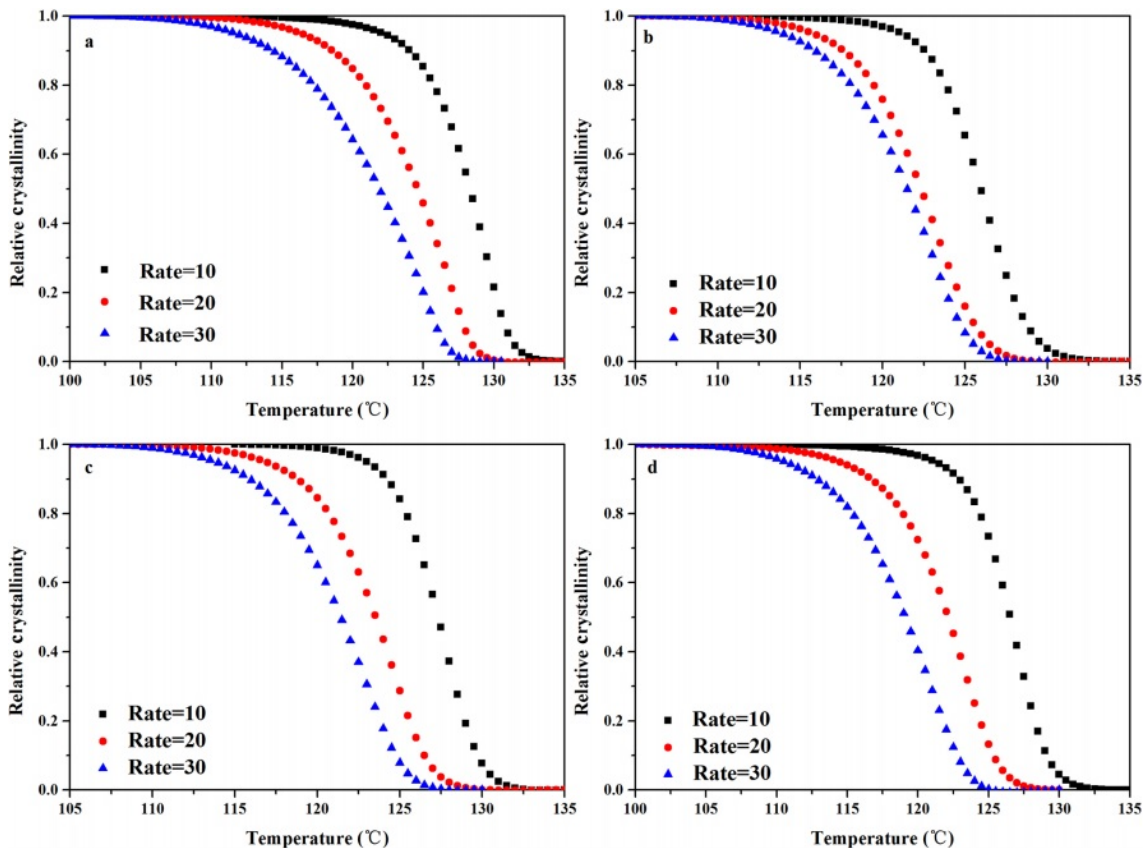


Figure 6. Non-isothermal crystallization relative crystallinity *versus* temperature of the rPP/ATP composites: (a) PP; (b) rPP; (c) rPP/3 wt% ATP; (d) rPP/3 wt% FATP.

where dH/dT is the crystallization heat flow rate at temperature T , T_0 represents the temperature at the start of crystallization, and T_∞ represents the temperature when crystallization was completed.³⁸

The data from Figure 5 was processed by eq. (1) and yielded the $X(t)$ versus temperature curves for different composites as Figure 6. By applying eq. (2), the $X(t)$ vs. crystallization time curves for different composites were obtained as Figure 7 and the data was recorded in Table 2.

$$t = (T_0 - T) / \phi \quad (2)$$

where the t is the crystallization time at temperature T , and the ϕ is the cooling rate.

It can be observed from Figure 7 and Table 2 that the half crystallization time ($t_{1/2}$) of the composites decreased with increased cooling rates. This was because rapid cooling caused insufficient time for the molecular chains of the composites to align in an ordered manner, initiating crystallization at lower temperatures and reducing the nucleation time and accelerating the crystallization process.³⁷ The $t_{1/2}$ of the rPP, rPP/3 wt% ATP, and rPP/3 wt% FATP at a rate of 10 °C/min were recorded as

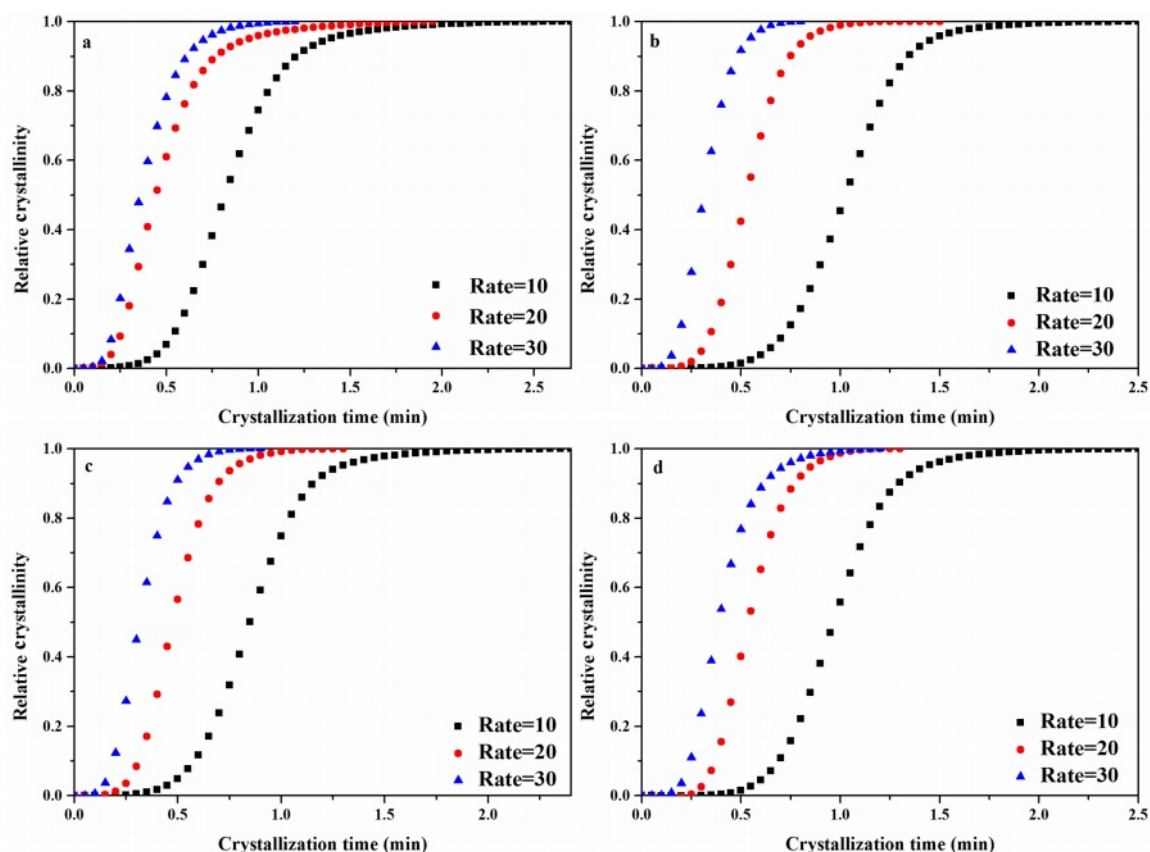


Figure 7. Non-isothermal crystallization relative crystallinity versus crystallization time of the rPP/ATP composites: (a) PP; (b) rPP; (c) rPP/3 wt% ATP; (d) rPP/3 wt% FATP.

2.23 min, 2.01 min, and 1.80 min and the rPP/3 wt% FATP composite can match the property of the PP. It can be demonstrated that the ATP can act as heterogeneous nucleating agent to reduce the time during random movement of molecular chains to form critical nuclei and increase the crystallization rate¹⁹ In addition, The MAFT in FATP can serve as internal lubricant in the rPP matrix, accelerating molecular chain movement, thereby further reducing the $t_{1/2}$ of the composites.

The *Avrami* equation which is used to study the crystallization kinetics of polymers is expressed as eq. (3):

$$\log[-\ln(1-X(t))] = n \log t + \log k \quad (3)$$

where $X(t)$ is obtained from eq. (1) and (2), n is the *Avrami* index, t is the crystallization time and k is the kinetic parameter.³⁹

The use of the *Avrami* equation for the study of non-isothermal crystallization kinetics has deviations, therefore, it is of great necessity to use the *Jeziorny* method to modify the *Avrami* equation. Based on the *Avrami* equation, the *Jeziorny* method can be employed to correct the k through ϕ by eq. (4) and

yielding the k_c . The $\log k_c$ is the crystallization rate constant.

$$\log k_c = (\log k)/\phi \quad (4)$$

The data from Figure 7 was processed by eq. (3) and (4) and yielded Figure 8, and the data from Figure 8 was recorded in Table 2. The increased $\log k_c$ indicated faster crystallization rate of the composites. The $\log k_c$ of different composites increased with the cooling rate increased. Under the same cooling rate, the $\log k_c$ of the composites increased with increased addition, and the rPP/3 wt% FATP composites exhibited the highest $\log k_c$. The above results supported the conclusion derived from the $t_{1/2}$ of the composites.

The n is linked to nucleation mechanisms and crystal growth patterns. The value represents the sum of the growth dimensionality of crystals and the time dimensionality of nucleation processes. When the growth dimensionality is 3, crystals exhibit spherical growth. In the case of heterogeneous nucleation, the time dimensionality is 0. The n of the rPP/ATP composites was around 3, indicating that the composites grown in the form of spherulites. This suggested that the ATP or FATP added in rPP

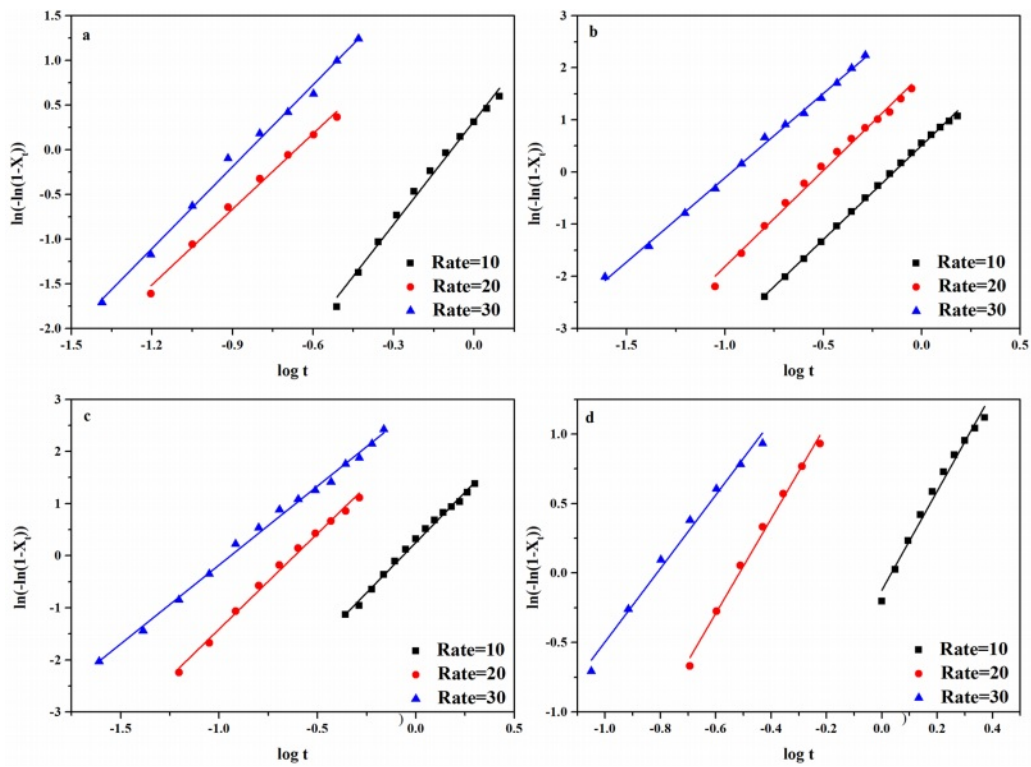


Figure 8. Non-isothermal crystallization kinetic curves of the rPP/ATP composites: (a) PP; (b) rPP; (c) rPP/3 wt% ATP; (d) rPP/3 wt% FATP.

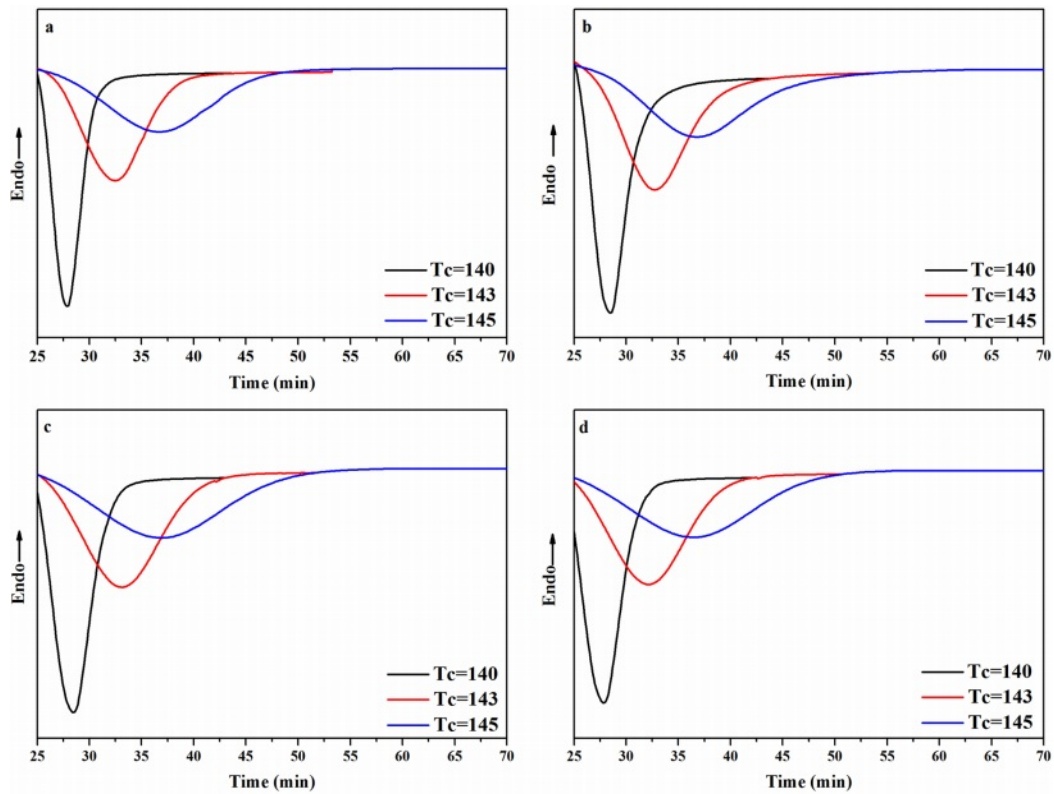


Figure 9. Isothermal crystallization curves of the rPP/FATP composites at different temperature: (a) PP; (b) rPP; (c) rPP/3 wt% ATP; (d) rPP/3 wt% FATP.

had no effect on the spherulites growth mode of the composites.

Isothermal Crystallization Behavior of the rPP/ATP Composites. The isothermal crystallization curves of the rPP/ATP composites at different temperatures were depicted in Figure 9. With decreased temperature, the crystallization peak of the composites narrowed, which indicated that the time for complete crystallization of the composites decreased. This was because the extended time for molecular chain rearrangement at lower temperatures and facilitating the formation of orderly crystalline structure. Consequently, the result led to an improvement in both the crystallization rate and the degree of the crystallization.⁴⁰

The data from Figure 9 processed by eq. (1) and yielded the $X(t)$ versus crystallization time curves for different composites as Figure 10, and the data was resulted in Table 3.

The result demonstrated from Figure 10 and Table 3 that under identical isothermal crystallization temperature, the trend of crystallization rate was as follows: rPP/3 wt% FATP < rPP/3 wt% ATP < rPP. For example, at the temperature of 140 °C, the $t_{1/2}$ of the rPP, rPP/3 wt% ATP, and rPP/3 wt% FATP were 2.88 min, 2.73 min, and 2.38 min, and the rPP/3 wt% FATP composite can match the property of the PP. This was because the ATP

Table 3. Isothermal Crystallization Kinetic Parameters of the rPP/ATP Composites

| Sample | T_c (°C) | n | $\log k_c$ | $t_{1/2}$ (min) |
|----------------|------------|------|------------|-----------------|
| PP | 140 | 2.49 | -3.056 | 2.37 |
| | 143 | 2.59 | -5.3366 | 6.82 |
| | 145 | 3.23 | -7.9327 | 10.39 |
| rPP | 140 | 1.86 | -2.3314 | 2.88 |
| | 143 | 2.31 | -4.9545 | 7.29 |
| | 145 | 2.35 | -6.0909 | 11.43 |
| rPP/3 wt% ATP | 140 | 2.18 | -3.1058 | 2.73 |
| | 143 | 2.43 | -5.4041 | 7.15 |
| | 145 | 2.67 | -7.3507 | 11.28 |
| rPP/3 wt% FATP | 140 | 2.73 | -4.0430 | 2.38 |
| | 143 | 3.17 | -7.6598 | 6.84 |
| | 145 | 3.41 | -8.6132 | 10.15 |

can reduce the time during the random movement of composites molecular chain to form critical nuclei, thereby increasing the isothermal crystallization rate. The MAFT in FATP can serve as internal lubricant, promoting the random movement of molecular chains, thereby further increasing the isothermal

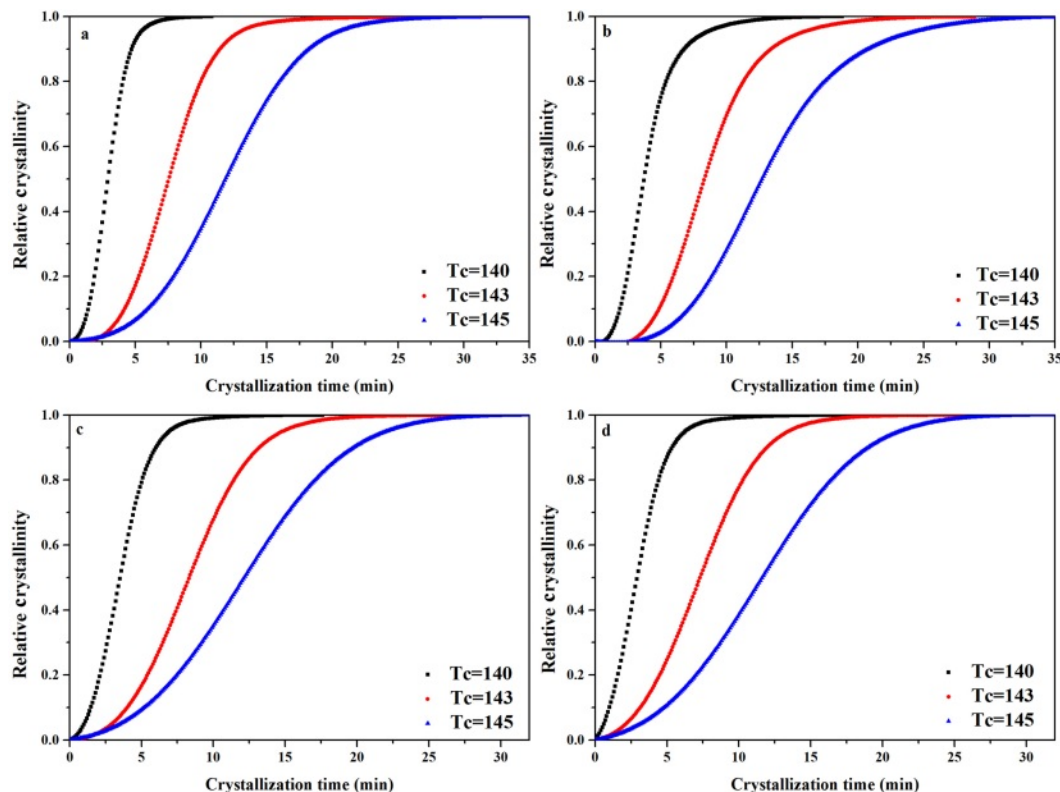


Figure 10. Isothermal crystallization relative crystallinity versus crystallization time of the rPP/ATP composites: (a) PP; (b) rPP; (c) rPP/3 wt% ATP; (d) rPP/3 wt% FATP.

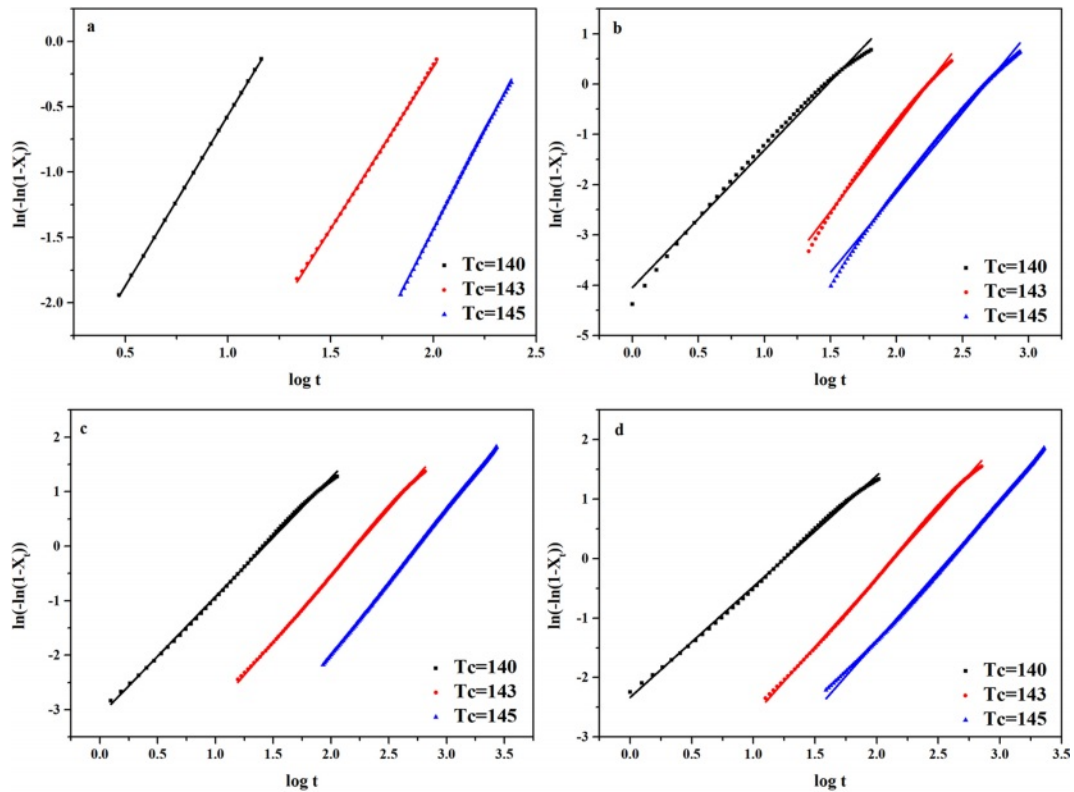


Figure 11. Isothermal crystallization kinetics curves of the rPP/FATP composites: (a) PP; (b) rPP; (c) rPP/3 wt% ATP; (d) rPP/3 wt% FATP.

crystallization rate.²⁸

Plotted $\log[-\ln(1-X(t))]-\log t$ according to eq. (3) and (4) yielded Figure 11 and the data was recorded in Table 3. As the crystallization temperature increased, the n slightly increased. This was because higher crystallization temperatures resulting in better crystals of the composites.

Furthermore, at the same crystallization temperature, the order of n was as follows: rPP < rPP/3 wt% ATP < PP < rPP/3 wt% FATP. The order corresponded to the trend of the $\log k_c$. The result demonstrated that reducing the polarity of the ATP through the MAFT improving the compatibility between ATP and rPP,

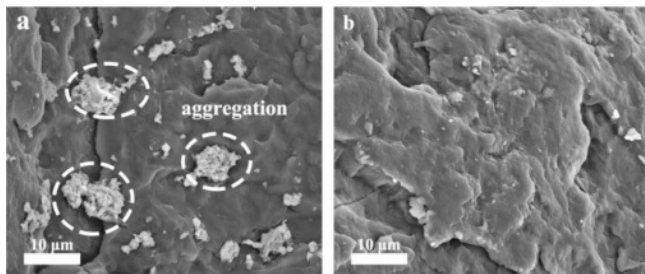


Figure 12. SEM photograph of the rPP/ATP composites: (a) rPP/3 wt% ATP; (b) rPP/3 wt% FATP.

leading to improve the crystallization of the rPP and beyond the level of the PP. The above results supported the conclusion derived from the isothermal crystallization $X(t)$ versus crystallization time of the composites.

Scanning Electron Microscopy Observations. Figure 12 showed the microstructure of the rPP/FATP composites. From the SEM images, it can be observed that the ATP exhibited significant aggregation within the rPP, indicating poor compatibility between ATP and rPP, thereby affecting the modification effect. The fracture surface of the rPP/3 wt% FATP composites appeared smoother with a noticeable improvement in the aggregation phenomenon. This suggested that the compatibility between ATP and rPP was significantly improved, which was also the fundamental reason for the superior crystallization and mechanical properties of the rPP/3 wt% FATP composites compared to the rPP/3 wt% ATP composites.

Conclusions

In this study, the ATP with unique one-dimensional rod-like structure was used to improve the mechanical and crystallization properties of the rPP. In order to increase the compatibility of

the polar ATP and the non-polar rPP, the MAH was grafted onto the FTW then reacted with ATP to prepare FATP. The rPP/ATP composites were prepared through melting blending. The mechanical properties demonstrated that the addition of the FATP improved the mechanical properties of the composites. Compared with rPP, the rPP/3 wt% FATP composites increased by 13.09%, 17.56%, and 101.92%, and reaching the level of the PP. Due to the improved compatibility, the mechanical properties of the rPP/FATP composites were increased compared with the rPP/ATP composites at the same addition. This was because the ATP can act as heterogeneous nucleating agent to promote the close packing of the composites molecular chains, thereby enhancing the mechanical properties of the composites. The MAFT can improve the compatibility between ATP and rPP and resulting ATP to disperse evenly within the rPP, thereby achieving better effects. Moreover, the DSC analysis proved that the addition of the ATP or FATP improved the crystallization properties of the rPP. The T_p of the rPP, rPP/3 wt% ATP, and rPP/3 wt% FATP was 126.31, 127.86, and 129.37 °C, respectively. The non-isothermal and isothermal crystallization kinetic results showed that the crystallization rate of the rPP was increased with the addition of the ATP and FATP. Meanwhile, by reason of the synergistic effect of compatibility improvement and internal lubrication, the crystallization rate of the rPP/FATP were faster than the rPP/ATP. This was because the ATP can reduce the time during the random movement of composites molecular chain to form critical nuclei, thereby increasing crystallization properties. The MAFT in FATP can serve as internal lubricant, promoting the random movement of molecular chains, thereby further increasing the crystallization properties. However, the ATP or FATP added in rPP had no effect on the spherulites growth mode of the composites. Above all, the SEM results provided intuitive evidence which the compatibility between FATP and rPP was greatly improved.

Acknowledgement: The authors acknowledge the financial support of the Scientific and Technological Innovation Programs of Higher Education Institutions in Shanxi (2023L421), the Special Project for Guiding the Transformation of Scientific and Technological Achievements of Shanxi Province (202204021301061), the Patent Transformation Special Plan Project of Shanxi Province (202303010), the Key Research and Development Project of Shanxi Province (202102040201004), the Graduate Joint Training Demonstration Base Project in Taiyuan University of Science and Technology (JD2022016).

Conflict of Interest: The authors declare that there is no conflict of interest.

References

1. Wang, B.; Zhang, H. R.; Huang, C.; Xiong, L.; Luo, J.; Chen, X. D. Mechanical and Rheological Properties of Isotactic Polypropylene/Bacterial Cellulose Composites. *Polym. Korea* **2017**, *41*, 460-464.
2. Ghanbari, A.; Seyedin, S.; Haddadi, S. A.; Nofar, M.; Ameli, A. Reinforcing Potential of Recycled Carbon Fibers in Compatibilized Polypropylene Composites. *J. Polym. Res.* **2021**, *28*, 145.
3. Roland, G.; Jambeck, J. R.; Lavender, L.K. Production, Use, and Fate of All Plastics Ever Made. *Sci. Adv.* **2017**, *3*, e1700782.
4. Phanthong, P.; Miyoshi, Y.; Yao, S. Development of Tensile Properties and Crystalline Conformation of Recycled Polypropylene by Re-Extrusion Using a Twin-Screw Extruder with an Additional Molten Resin Reservoir Unit. *Appl. Sci.* **2021**, *11*, 1707.
5. Prajapati, R.; Kohli, K.; Maity, S. K.; Sharma, B. K. *Recovery and Recycling of Polymeric and Plastic Materials*; Springer: Singapore, 2021.
6. Beltrán, F. R.; Barrio, L.; Lorenzo, V.; Río, B.; Martínez, U. J.; Orden, M. U. Valorization of Poly(lactic acid) Wastes via Mechanical Recycling: Improvement of the Properties of the Recycled Polymer. *Waste. Manag. Res.* **2018**, *37*, 135-141.
7. Shamsuyeva, M.; Endres H. J. Plastics in the Context of the Circular Economy and Sustainable Plastics Recycling: Comprehensive Review on Research Development, Standardization and Market. *Compos. Part C* **2021**, *6*, 100168.
8. Lee, A.; Liew, M. S. Tertiary Recycling of Plastics Waste: An Analysis of Feedstock, Chemical and Biological Degradation Methods. *J. Mater. Cycles. Waste. Manag.* **2021**, *23*, 32-43.
9. Yang, L.; Gao, J.; Liu, Y.; Zhuang, G.; Peng, X.; Wu, W. M.; Zhuang, X. Biodegradation of Expanded Polystyrene and Low-Density Polyethylene Foams in Larvae of *Tenebrio Molitor* Linnaeus (Coleoptera: Tenebrionidae): Broad Versus Limited Extent Depolymerization and Microbe-dependence versus Independence. *Chemosphere* **2021**, *262*, 127818.
10. Esmizadeh, E.; Tzoganakis, C.; Mekonnen, T. H. Degradation Behavior of Polypropylene during Reprocessing and Its Biocomposites: Thermal and Oxidative Degradation Kinetics. *Polymers* **2020**, *12*, 1627.
11. Martínez-Jothar, L.; Greenova, T. S.; Montes-Zavala, I.; Rivera-García, N.; Díaz-Ceja, Y.; Pérez, E.; Waldo-Mendoza, M. A. Thermal Degradation of Polypropylene Reprocessed in a Co-rotating Twin-screw Extruder: Kinetic Model and Relationship Between Melt Flow Index and Molecular weight. *Rev. Mex. Ing. Quim.* **2021**, *20*, 1079-1091.
12. Ragaert, K.; Delva, L.; Geem, K. V. Mechanical and Chemical Recycling of Solid Plastic Waste. *Waste. Manag. Res.* **2017**, *69*, 24-58.
13. Luna, C. B. B.; da Silva, W. A.; Araújo, E. M.; da Silva, L. J. M. D.; de Melo, J. B. D.A.; Wellen, R. M. R. From Waste to Potential Reuse:

- Mixtures of Polypropylene/Recycled Copolymer Polypropylene from Industrial Containers: Seeking Sustainable Materials *Sustainability* **2022**, 14, 6509.
14. Wei, J. J.; Duan, Y. J.; Wang, H.; Zhang, W. P. Study on Copolymerization Modification and Properties of Bio-based Trifunctional Diphenolic Acid Epoxy Resin by CE and DPR. *Polymer* **2023**, 284, 126308.
 15. Zúñiga, A.; Herrera, M. J.; Hernández, G. Impact Resistance Improvement on Modified Recycled PP using SBS and SEBS Elastomers. *Plast. Eng.* **2016**, 72, 36-37.
 16. Samat, N.; Lazim, N. H. M.; Motsidi, S. N. R. Performance Properties of Irradiated Recycled Polypropylene as a Compatibilizer in Recycled Polypropylene/Microcrystalline Cellulose *Compos. Mater. Sci. Forum.* **2017**, 894, 62-65.
 17. Sahin, M.; Schlögl, S.; Kalinka, G.; Wang, J. P.; Kaynak, B.; Mühlbacher, I.; Ziegler, W.; Kern, W.; Grützmacher, H. Tailoring the Interfaces in Glass Fiber-Reinforced Photopolymer Composites. *Polymer* **2018**, 141, 221-231.
 18. Lovette, M. A.; Browning, A. R.; Griffin, D. W.; Sizemore, J. P.; Snyder, R. C.; Doherty, M. F. Crystal Shape Engineering. *Ind. Eng. Chem. Res.* **2008**, 47, 9812-9833.
 19. Hou, F. Open Questions on Physical Chemistry of Crystal Growth from Congruent Melts. *Commun. Chem.* **2021**, 4, 131.
 20. Tsou, C. H.; Zeng, R.; Tsou, C. Y.; Chen, J. C.; Sun, Y. L.; Ma, Z. L.; De Guzman, M. R.; Tu, L. J.; Tian, X. Y.; Wu, C. S. Mechanical, Hydrophobic, and Barrier Properties of Nanocomposites of Modified Polypropylene Reinforced with Low-Content Attapulgite. *Polymers* **2022**, 14, 3696.
 21. Wang, L. H.; Sheng, J.; Wu, S. Z. Isothermal Crystallization Kinetics of Polypropylene/Attapulgite Nanocomposites. *J. Macromol. SCI. B.* **2004**, 43, 935-946.
 22. Chen, J. J.; Chen, J. Y.; Zhu, S. P.; Cao, Y.; Li, H. L. Mechanical Properties, Morphology, and Crystal Structure of Polypropylene/Chemically Modified Attapulgite Nanocomposites. *J. Appl. Polym. Sci.* **2011**, 121, 899-908.
 23. Tsiptsias, C.; Leontiadis, K.; Messaritakis, S.; Terzaki, A.; Xidas, P.; Mystikos, K.; Tzimpilis, E.; Tsvintzelis, I. Experimental Investigation of Polypropylene Composite Drawn Fibers with Talc, Wollastonite, Attapulgite and Single-Wall Carbon Nanotubes. *Polymers* **2022**, 14, 260.
 24. Yuan, W. J.; Wang, F.; Gao, C.; Liu, P.; Ding, Y. F.; Zhang, S. M.; Yang, M. S. Enhanced Foamability of Isotactic Polypropylene/Polypropylene-grafted-Nanosilica Nanocomposites in Supercritical Carbon Dioxide. *Polym. Eng. Sci.* **2020**, 60, 1353-1364.
 25. Ndiaye, D.; Tidjani, A. Effects of Coupling Agents on Thermal Behavior and Mechanical Properties of Wood Flour/Polypropylene Composites. *J. Compos. Mater.* **2012**, 46, 3067-3075.
 26. Rathnayake, W. S. M.; Karunanayake, L.; Samarasekara, A. M. P. B.; Amarasinghe, D. A. S. Sunflower Oil-Based MCC Surface Modification to Achieve Improved Thermomechanical Properties of a Polypropylene Composite. *Cellulose* **2020**, 27, 4355-4371.
 27. Karaba, A.; Rozhon, J.; Patera, J.; Hájek, J.; Zámotny, P. Fischer-Tropsch Wax from Renewable Resources as an Excellent Feedstock for the Steam-Cracking Process. *Chem. Eng. Technol.* **2021**, 44, 329-338.
 28. Hawley G. Hawley's Condensed Chemical Dictionary. *Soil. Sci.* **1943**, 14, 592-593.
 29. Mao, S. D.; Zhang, M.; Lin, F. H.; Li, X. Y.; Zhao, Y. Y.; Zhang, Y. L.; Gao, Y. F.; Luo, J.; Chen, X. D.; Wang, B. Attapulgite Structure Reset to Accelerate the Crystal Transformation of Isotactic Polybutene. *Polymers* **2022**, 14, 3820.
 30. Papageorgiou, D. G.; Kinloch, I. A.; Young, R. J. Mechanical Properties of Graphene and Graphene-based Nanocomposites. *Prog. Mater. Sci.* **2017**, 90, 75-127.
 31. Ezenkwa, O. E.; Hassan, A.; Samsudin, S. A.; Comparison of Mechanical Properties and Thermal Stability of Graphene-based Materials and Halloysite Nanotubes Reinforced Maleated Polymer Compatibilized Polypropylene Nanocomposites. *Polym. Compos.* **2022**, 43, 1852-1863.
 32. Wang, B.; Nie, K.; Xue, X. R.; Lin, F. H.; Li, X. Y.; Xue, Y. B.; Luo, J. Preparation of Maleic Anhydride Grafted Polybutene and Its Application in Isotactic Polybutene-1/Microcrystalline Cellulose Composites. *Polymers* **2018**, 10, 393.
 33. He, L. P.; Li, W. J.; Chen, D. C.; Zhou, D. W.; Lu, G.; Yuan, J. M. Effects of Amino Silicone Oil Modification on Properties of Ramie Fiber and Ramie Fiber/Polypropylene Composites. *Mater. Design* **2015**, 77, 142-148.
 34. Zuiderduin, W. C. J.; Westzaan, C.; Huétink, J.; Gaymans, R. J. Toughening of Polypropylene with Calcium Carbonate Particles. *Polymer* **2003**, 44, 261-275.
 35. Kiziltas, A.; Gardner, D. J.; Han, Y.; Yang, H. S. Determining the Mechanical Properties of Microcrystalline Cellulose (MCC)-filled PET-PTT Blend Composites. *J. Polym. Environ.* **2010**, 42, 165-176.
 36. Li, F. S.; Gao, Y. B.; Jiang, W. Design of High Impact Thermal Plastic Polymer Composites with Balanced Toughness and Rigidity: Toughening with One Phase Modifier. *Polymer* **2019**, 170, 101-106.
 37. Sattaria, M.; Molazemhosseini, A.; Naimi-Jamal, M. R.; Khavandi, A. Nonisothermal Crystallization Behavior and Mechanical Properties of PEEK/SCF/Nano-SiO₂ Composites. *Mater. Chem. Phys.* **2014**, 147, 942-953.
 38. Kwon, S.; Zhang, T.; Jang, Y.; Jung, M.; Lee, E.; Kang, H. J. Non-isothermal Crystallization of Poly(3-hydroxybutyrate-co-4-hydroxybutyrate). *Ploy. Korea* **2022**, 46, 661-670.
 39. Lee, J. I.; Bae, J. W.; Kim, S. L.; Hong, J. E.; Nam, B. U. Study on Impact Resistance, Wear Resistance and Crystallization Kinetics of Polypropylene Modified by Complex Crosslinkers. *Ploy. Korea* **2020**, 44, 603-609.
 40. Citrawati, F.; Quadir, M. Z.; Munroe, P. R. Effect of Heating Rate and Annealing Temperature on Secondary Recrystallization of Goss Grains in a Grain Orientated Silicon Steel. *ISIJ. Int.* **2017**, 57, 1112-1200.
- Publisher's Note** The Polymer Society of Korea remains neutral with regard to jurisdictional claims in published articles and institutional affiliations.